Kinetostatic Analysis of Underactuated Fingers

Lionel Birglen, *Student Member, IEEE,* and Clément M. Gosselin, *Member, IEEE*

***Abstract*—The aim of this paper is to establish a fundamental basis for the analysis of underactuated fingers with a general approach. A new method to obtain the force capabilities of *any* underactuated fingers will be presented. Force capability is defined as the ability to generate an external wrench onto a fixed object with a given set of phalanges. This method is based on the introduction of two new matrices which completely describe the relationship between the input torque of the finger actuator(s) and the contact forces on the phalanges. Using this tool, one can study the conditions under which certain phalanx forces vanish, and compare different underactuation mechanisms with a rigorous approach.**

***Index Terms*—Robot hand, shape adaptation, stable grasp, underactuation.**

I. Introduction

ROBOTIC hands have been developed with the aim of matching the human hand in terms of dexterity and adaptation capabilities to equip either a dextrous manipulator or a human being as a prosthetic device. Pioneer designs include: the Okada hand [1], the Stanford/JPL (Salisbury's) hand [2], the Utah/MIT hand [3], the Belgrade/USC hand [4], the BarrettHand [5], the hands from the DLR [6], [7], the LMS hand [8], or the NASA Robonaut hand [9]. However, significant efforts have been made to find designs simple enough to be easily built and controlled, in order to obtain practical systems [10], [11], particularly in human prosthetics. To overcome the mitiged success of the early designs, mainly due to the cost of the control architecture needed for complex mechanical systems with often more than ten actuators plus many sensors, a special emphasis has been placed on the reduction of the number of degrees of freedom (DOFs), thereby decreasing the number of actuators. In particular, the SSL hand [12], the Graspar hand [13], the DIES-DIEM hand [14], the Cassino finger [15], and the TBM hand [16] have followed this path. On the other hand, very few prototypes involve a smaller number of actuators without decreasing the number of DOFs. This approach, namely, *underactuation*, can be implemented through the use of passive elements like springs or mechanical limits leading to a mechanical adaptation of the finger to the shape of the object to be grasped [17]–[22]. A similar approach consists of using elastic phalanges, which increase the adaptation capability but decrease considerably the strength of the grasp [23], [24]. Another way to consider shape adaptation is to use tentacle-like fingers [25].

Two main approaches dominate the literature on robotic grasping. On one hand, purely theoretical work on grasping and manipulation and, on the other hand, the rather intuitive design of functional prototypes. This paper is an attempt to bridge this gap, for the special case of underactuated fingers. Indeed, if the development of underactuated fingers aims at overcoming the theoretical difficulties of general manipulation issues, and at obtaining prototypes of practical utility, the capabilities of these fingers remain not well known. Prototypes have often been built with intuitive design, without a generic knowledge of the resulting behavior, and based mainly on specific computer-aided simulation. This paper presents an effort to establish a common framework using simple theoretical bases. The fundamental goal of underactuation being simplicity, the objective of this paper is to provide practical tools for the analysis and comparison of underactuated fingers. Indeed, some issues have been overlooked in previous work and should be systematically addressed; for instance, the grasp force distribution, the capability of the finger to actually exert forces on a grasped object, the stability of the grasp, etc. Underactuation in robotic hands generates intriguing properties. For example, such hands cannot always ensure full *whole-hand grasping*. Indeed, the distribution of the forces onto the different phalanges is partially predetermined by the mechanical design of the hand, and some phalanges may not be able to actually exert any effort in certain configurations. This uncontrollable force distribution can also lead to unstable grasps, a continuous closing motion of the actuator tending to eject the object. In [26], the authors have presented a brief illustration of the above issues for a 2-DOF finger. The latter reference can be seen as a more detailed introduction of this paper, which generalizes the work to n-DOF fingers with a general architecture. Hence, the paper [26] will be often referred to. A new method to study the capabilities of underactuated fingers will be presented that allows rigorous comparison of different transmission mechanisms through the definition of different indexes, similar to the dexterity in kinematic analysis. In this paper:

- two matrices that completely define the contact forces as a function of the actuator(s) torque(s) are defined;
- using these matrices, configurations of the finger leading to stable grasps are presented;
- indexes to quantify the ability of the finger to create these stable grasps are introduced;
- different mechanisms used in underactuated hands are compared, using the latter indexes;
- finally, considerations on other aspects not covered in this paper are discussed.

Manuscript received November 18, 2002; revised February 26, 2003. This paper was recommended for publication by Associate Editor C. Melchiorri and Editor I. Walker upon evaluation of the reviewers' comments. This work was supported in part by Natural Sciences and Engineering Research of Canada (NSERC) and in part by the Canada Research Chair Program.

The authors are with the Department of Mechanical Engineering, Laval University, Québec, QC G1K 7P4, Canada (e-mail: birgle00@gmc.ulaval.ca; gosselin@gmc.ulaval.ca).

Digital Object Identifier 10.1109/TRA.2004.824641

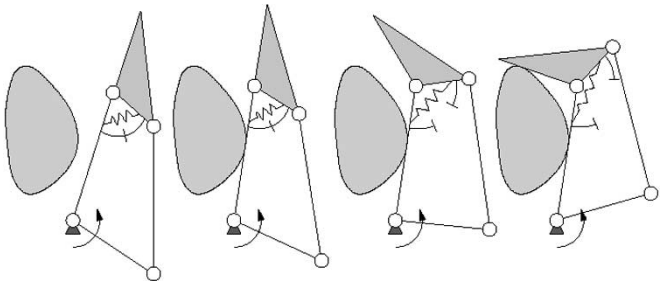

Fig. 1. Closing sequence of a 2-DOF underactuated finger, courtesy of Thierry Laliberté, modified with permission.

The first part of the paper (Section III) establishes the fundamental background of our analysis and requires knowledge of screw theory and mechanical transmission design. This is the theoretical aspect of our work. One then illustrates in the second part (Sections IV and V), how these results can be used to design and characterize underactuated fingers. Sections IV and V represent the practical aspect of the paper.

II. Underactuation in Robotic Hands

Underactuation in robotic fingers is different from the concept of underactuation usually presented in robotic systems, and these notions should not be confused. An underactuated robot is generally defined as a manipulator with one or more unactuated joints. On the other hand, underactuated fingers generally use elastic elements in the design of their "unactuated" joints. Thus, one should rather think of these joints as uncontrollable or passively driven instead of unactuated. In an underactuated finger, the actuation wrench T_a is applied to the input of the finger and is transmitted to the phalanges through suitable mechanical design, e.g., four-bar linkages, pulleys and tendons, gears, etc. Since underactuated fingers have many DOFs, say n, and fewer than n actuators, passive elements are used to kinematically constrain the finger and ensure the shape adaptation of the finger to the object grasped. To this end, springs and mechanical limits are often used, though inertial properties of the mechanism can also be used [13]. An example of an underactuated 2-DOF finger using linkages and its closing process is illustrated in Fig. 1. Notice the mechanical limit that allows a preloading of the spring to prevent any undesirable motion of the second phalanx due to its own weight and/or inertial effects, and also to prevent hyperflexion of the finger. Springs are useful for keeping the finger from incoherent motion, but when the grasp sequence is complete, they still oppose the actuator force. Thus, springs shall be designed with the smallest stiffness possible, however, sufficient to keep the finger from collapsing.

III. N-DOF 1-DOA Finger

A. Introduction

A general n-DOF, 1-degree-of-actuation (DOA) finger with four-bar linkages will be considered for initial analysis. If, usually, only three phalanges are used in robotic fingers, the results presented here can be extended to other mechanical devices using underactuation, such as elephant trunks or snake-like robots. Indeed, one of the first underactuated grippers consisted

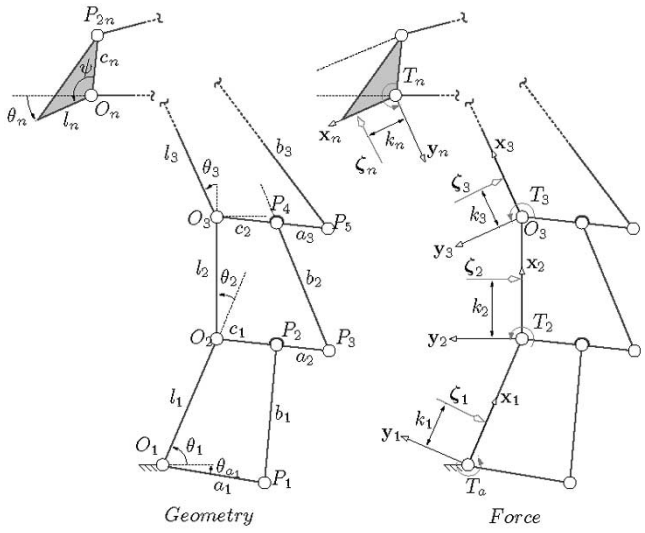

Fig. 2. Model of underactuated n-DOF finger: geometric and force parameters.

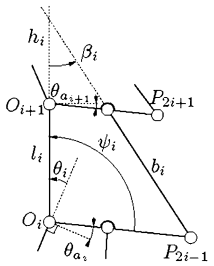

Fig. 3. Detailed modeling of a single stage of the finger.

of two ten-phalanx fingers [17]. Results will be subsequently extended to more general types of transmission. This design is a generalized version of the three-phalanx finger used in the Mars and Sarah prototypes [27], hence, more detailed results for $n = 2$ and $n = 3$ will also be given. The model of the finger is presented in Fig. 2, more details about a single stage are found in Fig. 3. Note that the finger is planar, i.e., abduction/adduction is not considered. Indeed, such motions are generally not used during the final grasp, but rather for reconfiguration of the finger or manipulation. Moreover, contacts happen not only with the fingertip but with all phalanges, the finger being designed for grasping and not for dextrous manipulation.

In order to determine the configurations where the finger can apply forces to the object grasped, one shall proceed with a quasi-static modeling of the finger. Equating the input and the output virtual powers, one obtains

$$\mathbf{t}^T \boldsymbol{\omega}_a = \mathbf{f}^T \mathbf{v} \tag{1}$$

where $\mathbf{t}$ is the input torque vector exerted by the actuator and the springs, $\boldsymbol{\omega}_a$ is the corresponding velocity vector, $\mathbf{f}$ is the vector of contact wrenches, and $\mathbf{v}$ is the vector containing the twist of each of the contact points, i.e.,

$$\mathbf{t} = \begin{bmatrix} T_a \\ T_2 = -K_2 \Delta\theta_2 \\ T_3 = -K_3 \Delta\theta_3 \\ \cdots \\ T_n = -K_n \Delta\theta_n \end{bmatrix} \quad \boldsymbol{\omega_a} = \begin{bmatrix} \dot{\theta}_{a_1} \\ \dot{\theta}_2 \\ \dot{\theta}_3 \\ \cdots \\ \dot{\theta}_n \end{bmatrix} \tag{2}$$

where K_i is the stiffness of the torsional spring located at point O_i. One also has

$$\mathbf{f} = \begin{bmatrix} \boldsymbol{\zeta}_1\diamond \\ \boldsymbol{\zeta}_2\diamond \\ \boldsymbol{\zeta}_3\diamond \\ \dots \\ \boldsymbol{\zeta}_n\diamond \end{bmatrix} \quad \mathbf{v} = \begin{bmatrix} \boldsymbol{\xi}_1 \\ \boldsymbol{\xi}_2 \\ \boldsymbol{\xi}_3 \\ \dots \\ \boldsymbol{\xi}_n \end{bmatrix} \tag{3}$$

where $\boldsymbol{\zeta}_i\diamond$ is a shorthand notation of the wrench $\boldsymbol{\zeta}_i = [f_i^x \; f_i^y \tau_i]^T$ where the moment has been written before the force coordinates [28]. $\boldsymbol{\xi}_i = [\omega_i \; v_i^x \; v_i^y]^T$ is the twist of the ith contact point. The contact twist can be simply expressed as the product of a Jacobian matrix $\mathbf{J}$ and the derivatives of the phalanx joint coordinates, which is a natural choice, i.e., $\mathbf{v} = \mathbf{J}\dot{\boldsymbol{\theta}}$ with $\boldsymbol{\theta} = [\theta_1\theta_2 \dots \theta_n]^T$. Similarly, one can also establish the matrix $\mathbf{T}$ which relates the vector $\boldsymbol{\omega_a}$ to the derivatives of the phalanx joint coordinates, and contains the elements function of the transmission mechanisms used, i.e., $\dot{\boldsymbol{\theta}} = \mathbf{T}\boldsymbol{\omega_a}$. Equation (1) then becomes

$$\mathbf{t}^T\mathbf{T}^{-1} = \mathbf{f}^T\mathbf{J}. \tag{4}$$

However, one should remember that matrix $\mathbf{J}$ is generally not square. Therefore, $\mathbf{f}$ is not unique for a given $\mathbf{t}$, even if Coulomb friction is considered, an infinite number of wrenches satisfy (4) if $\mathbf{J}$ is of rank $r > n$. Indeed, the general solution of (4) is of the form

$$\mathbf{f} = \mathbf{J}^{T+}\mathbf{T}^{-T}\mathbf{t} + (\mathbf{1}_{3n} - \mathbf{J}^{T+}\mathbf{J}^T)\mathbf{z} \tag{5}$$

where $\mathbf{z} \in \mathbb{R}^{3n}$ and $\mathbf{J}^{T+}$ is the pseudoinverse of matrix $\mathbf{J}^T$. On the other hand, for a given $\mathbf{f}$, $\mathbf{t}$ is uniquely defined by (4). To obtain a bijective relationship between $\mathbf{t}$ and $\mathbf{f}$, each contact wrench will be assumed to be a pure force normal to the phalanx, i.e., $\boldsymbol{\zeta}_k = f_k\mathbf{y}_k^\star$, where $\mathbf{y}_k^\star = [\mathbf{y}_k^T \quad 0]^T$ is the unit wrench corresponding to a pure force along $\mathbf{y}_k$, where $\mathbf{y}_k$ is a unit vector orthogonal to the kth phalanx. This assumption can seem very restrictive. However, our primary aim is to study the capability of *the finger (and only the finger)* to exert a wrench onto a fixed object. We are, therefore, not interested in the local properties of the contact, such as friction or geometry of the contact. In order to obtain simple and general results that can characterize the finger itself and not the system formed by the finger and the object, pure normal forces should be considered. Obviously, the omitted local properties can have a tremendous impact in terms of stability of the grasp but exceed the scope of this paper. Therefore, one shall modify vector $\mathbf{f}$ and $\mathbf{v}$ as

$$\mathbf{f} = \begin{bmatrix} f_1 \\ f_2 \\ f_3 \\ \dots \\ f_n \end{bmatrix} \quad \mathbf{v} = \begin{bmatrix} \boldsymbol{\xi}_1 \circ \mathbf{y}_1^\star \\ \boldsymbol{\xi}_2 \circ \mathbf{y}_2^\star \\ \boldsymbol{\xi}_3 \circ \mathbf{y}_3^\star \\ \dots \\ \boldsymbol{\xi}_n \circ \mathbf{y}_n^\star \end{bmatrix} \tag{6}$$

where the operator $\circ$ stands for the reciprocal product of screws in the plane. Thus, $\mathbf{f}$ is the vector of contact force magnitudes, and $\mathbf{v}$ is the vector of the projections of the contact twists onto the respective normals of the phalanges. One shall now proceed with the definition of matrices $\mathbf{J}$ and $\mathbf{T}$ corresponding to the updated expressions of $\mathbf{f}$ and $\mathbf{v}$ defined in (6). One shall keep in mind that the expression of matrix $\mathbf{J}$ is modified so that $\mathbf{v} = \mathbf{J}\dot{\boldsymbol{\theta}}$ is preserved with (6). The twist at the kth contact point is given by

$$\boldsymbol{\xi}_k = \sum_{i=1}^{k} \dot{\theta}_i \boldsymbol{\xi}_k^{O_i} \tag{7}$$

where $\boldsymbol{\xi}_k = (\omega_k, v_k^x, v_k^y)$ and $\boldsymbol{\xi}_k^{O_i}$ is the joint twist associated to O_i with respect to the contact point considered [29]. The latter can be written as

$$\boldsymbol{\xi}_k^{O_i} = \begin{bmatrix} \mathbf{1} \\ \mathbf{E}\mathbf{r}_{ik} \end{bmatrix} \tag{8}$$

since every joint between two phalanges is assumed to be of the revolute type, and where $\mathbf{r}_{ik}$ is the vector from O_i to the contact point on the kth phalanx. $\mathbf{E}$ is the matrix representation of the cross product in the plane, i.e.,

$$\mathbf{E} = \begin{bmatrix} 0 & -1 \\ 1 & 0 \end{bmatrix}. \tag{9}$$

Thus, the virtual power $\boldsymbol{\zeta}_k \circ \boldsymbol{\xi}_k$ can be expressed as

$$\boldsymbol{\zeta}_k \circ \boldsymbol{\xi}_k = f_k\mathbf{y}_k^\star \circ \left(\sum_{i=1}^{k} \dot{\theta}_i \boldsymbol{\xi}_k^{O_i} \right) = f_k \sum_{i=1}^{k} \dot{\theta}_i \mathbf{y}_k^\star \circ \boldsymbol{\xi}_k^{O_i} \tag{10}$$

therefore, finally

$$\boldsymbol{\zeta}_k \circ \boldsymbol{\xi}_k = f_k \sum_{i=1}^{k} \dot{\theta}_i \mathbf{r}_{ik}^T \mathbf{E}^T \mathbf{y}_k = f_k \sum_{i=1}^{k} \dot{\theta}_i \mathbf{r}_{ik}^T \mathbf{x}_k \tag{11}$$

where $\mathbf{x}_k$ is a unit vector tangent to the kth phalanx. With $\mathbf{v} = \mathbf{J}\dot{\boldsymbol{\theta}}$, one can finally obtain the matrix $\mathbf{J}$ in a lower triangular form

$$\mathbf{J} = \begin{bmatrix} k_1 & 0 & 0 & \dots & 0 \\ \mathbf{r}_{12}^T\mathbf{x}_2 & k_2 & 0 & \dots & 0 \\ \dots & \dots & \dots & \dots & \dots \\ \mathbf{r}_{1n}^T\mathbf{x}_n & \mathbf{r}_{2n}^T\mathbf{x}_n & \mathbf{r}_{3n}^T\mathbf{x}_n & \dots & k_n \end{bmatrix} \tag{12}$$

noticing that $\mathbf{r}_{ii}^T\mathbf{x}_i = k_i$. The elements of the matrix can be given explicitly as

$$\mathbf{r}_{ij}^T\mathbf{x}_j = k_j + \sum_{k=i}^{j-1} l_k \cos\left(\sum_{m=k+1}^{j} \theta_m \right), \quad i < j. \tag{13}$$

Note that the expression of matrix $\mathbf{J}$ is not specific to underactuated fingers and still holds in more general cases, provided that abduction/adduction is not considered. One can also establish the matrix $\mathbf{T}$, which relates the vector $\boldsymbol{\omega_a}$ to the derivatives of the phalanx joint coordinates, i.e., $\dot{\boldsymbol{\theta}} = \mathbf{T}\boldsymbol{\omega_a}$ or

$$\begin{bmatrix} \dot{\theta}_1 \\ \dot{\theta}_2 \\ \dot{\theta}_3 \\ \dots \\ \dot{\theta}_n \end{bmatrix} = \begin{bmatrix} X_1 & X_2 & X_3 & \dots & X_n \\ 0 & 1 & 0 & \dots & 0 \\ 0 & 0 & 1 & \dots & 0 \\ \dots & \dots & \dots & \dots & \dots \\ 0 & 0 & 0 & \dots & 1 \end{bmatrix} \begin{bmatrix} \dot{\theta}_{a_1} \\ \dot{\theta}_2 \\ \dot{\theta}_3 \\ \dots \\ \dot{\theta}_n \end{bmatrix}. \tag{14}$$

Note that the form of this matrix is characteristic of underactuation. If the finger is fully actuated, $\mathbf{T}$ should be the identity matrix of dimension n. Also, X_i is a function of the linkage used to transmit the actuator torque to the ith phalanx. The linkage used in our model is most common, since it allows both compactness and simplicity. For the model discussed here, the principle of transmission gives the angular velocity ratio of a four-bar linkage, also known as *Kennedy's Theorem* [30], [31] (consider

$O_{i-1}O_iP_{2i-2}P_{2i-3}$ with θ_{i-1} constant) and by superposition, one obtains

$$\dot{\theta}_{a_{i-1}} = \dot{\theta}_{i-1} + \frac{h_i}{h_i + l_{i-1}}\dot{\theta}_{a_i} \tag{15}$$

since the velocity output of each stage is the input of the next stage, where

$$h_i = c_{i-1}(\cos(\theta_i - \psi_i) - \sin(\theta_i - \psi_i)\cot\beta_{i-1}) \tag{16}$$

is the signed distance between point O_i and the geometric intersection of lines $(O_{i-1}O_i)$ and $(P_{2i-2}P_{2i-3})$. This distance can be negative if the intersection point is on the same side as O_{i-1} with respect to O_i. Thus, $h_i + l_{i-1}$ can also vanish. Geometrically, it corresponds to the case where links a_{i-1} and b_{i-1} are aligned. In such a configuration, it is easy to see that power cannot be properly transmitted, and infinitesimal motion $\Delta\theta_{a_{i-1}}$ is possible with $\Delta\theta_{a_i} = 0$. One can also obtain $\cot\beta_{i-1}$ as a function of the parameters of the system, i.e.,

$$\frac{c_{i-1}S_{\theta_i-\psi_i}\sqrt{4a_{i-1}^2b_{i-1}^2 - N_i^2} + M_i(l_{i-1} + c_{i-1}C_{\theta_i-\psi_i})}{-(l_{i-1} + c_{i-1}C_{\theta_i-\psi_i})\sqrt{4a_{i-1}^2b_{i-1}^2 - N_i^2} + M_ic_{i-1}S_{\theta_i-\psi_i}} \tag{17}$$

where S_α and C_α stand, respectively, for $\sin\alpha$ and $\cos\alpha$, and with

$$\begin{aligned} M_i =& -l_{i-1}(l_{i-1} + 2c_{i-1}\cos(\theta_i - \psi_i)) \\ &+ a_{i-1}^2 - b_{i-1}^2 - c_{i-1}^2 \\ N_i =& \, l_{i-1}(l_{i-1} + 2c_{i-1}\cos(\theta_i - \psi_i)) \\ &- a_{i-1}^2 - b_{i-1}^2 + c_{i-1}^2 \end{aligned}$$

where ψ_i can be expressed as a function of ψ_{i-1} and θ_i, thus one can obtain the expressions of each ψ_i recursively. Equation (15) can be used recursively to obtain $\dot{\theta}_{a_1}$ as a function of vector $\dot{\boldsymbol{\theta}}$, i.e.,

$$\begin{aligned} \dot{\theta}_{a_1} =& \dot{\theta}_1 + \frac{h_2}{h_2 + l_1}\dot{\theta}_{a_2} \\ =& \dot{\theta}_1 + \frac{h_2}{h_2 + l_1}\left(\dot{\theta}_2 + \frac{h_3}{h_3 + l_2}\dot{\theta}_{a_3}\right) \\ =& \ldots \end{aligned} \tag{18}$$

also, for the last phalanx

$$\dot{\theta}_{a_n} = \dot{\theta}_{n-1} + \frac{h_n}{h_n + l_{n-1}}\dot{\theta}_n \tag{19}$$

one obtains

$$\dot{\theta}_{a_1} = \dot{\theta}_1 + \frac{h_2}{h_2 + l_1}\dot{\theta}_2 + \cdots + \prod_{i=2}^{n}\frac{h_i}{h_i - l_{i-1}}\dot{\theta}_n \tag{20}$$

and, by identification between (20) and (14), one finally has

$$\mathbf{T}^T = \begin{bmatrix} 1 & \mathbf{0}_{n-1}^T \\ -\dfrac{h_2}{h_2 + l_1} & \\ -\dfrac{h_2h_3}{(h_2 + l_1)(h_3 + l_2)} & \\ \cdots & \mathbf{1}_{n-1} \\ -\displaystyle\prod_{i=2}^{n}\frac{h_i}{h_i + l_{i-1}} & \end{bmatrix} \tag{21}$$

where $\mathbf{1}_{n-1}$ and $\mathbf{0}_{n-1}$ are, respectively, the identity matrix and the zero vector of dimension $n-1$. This method can also be used to obtain elements of matrix $\mathbf{T}$ with different types of transmission mechanisms. Examples will be given in Section IV. Finally, one obtains

$$\mathbf{f} = \mathbf{J}^{-T}\mathbf{T}^{-T}\mathbf{t} \tag{22}$$

which is the equation that provides a practical relationship between the actuator torques and contact forces. One can note that $\mathbf{T}^{-T} = -\mathbf{T}^T + 2\mathbf{1}_n$, thus this inverse is not computationally intensive, and specific inversion procedures exist for triangular matrices. This formulation is, therefore, very well suited for both analytical derivations and numerical calculations. Furthermore, if the finger is fully actuated, i.e., $\mathbf{T} = \mathbf{1}_n$, one has $\mathbf{f} = \mathbf{J}^{-T}\mathbf{t}$, a relationship similar to the grasp matrix linking fingertips to object wrenches or the Jacobian matrix that maps joint torques to fingertip forces, both usually presented in grasping papers [32], [33]. As for the validity of this equation, conditions for existence of the inverses are

$$\det(\mathbf{T}) = 1 \neq 0 \tag{23}$$

$$\det(\mathbf{J}) = \prod_{i=1}^{n} k_i \neq 0 \tag{24}$$

which means that contacts should exist with all phalanges, and that $\mathbf{T}$ should exist, i.e.,

$$\prod_{i=2}^{n}(h_i + l_{i-1}) \neq 0. \tag{25}$$

meaning geometrically that points O_i, P_{2i-2}, and P_{2i-3} are not on the same line. If this is not true, no effort can be transmitted to upper stages of the mechanism in the current configuration. Another interesting case arises if $h_k = 0$, then $X_j = 0,\ j \geq k$ because of the particular form of the coefficient X_j

$$X_j = -\prod_{i=2}^{j}\frac{h_i}{h_i + l_{i-1}}, \quad j > 1 \quad \text{and} \quad X_1 = 1. \tag{26}$$

This has a simple physical interpretation: $h_k = 0$ means that the distance between point O_k and the geometric intersection of lines $(O_{k-1}O_k)$ and $(P_{2k-2}P_{2k-3})$ is zero. Thus, both lines intersect in O_k. If one assumes that $c_{k-1} \neq 0$, it means that points O_k, P_{2k-2}, and P_{2k-3} are on the same line. Since the actuator torque is usually transmitted to upper stages of the mechanism through link b_{k-1}, and that in this particular configuration, such transmission is impossible (link b_{k-1} cannot generate any actuation torque about O_k), no motion is transmitted, hence, no torque except for the springs, which are usually negligible. Consequently, an infinitesimal rotation is possible around O_k, and if the springs are neglected, one also has that $f_j = 0,\ j \geq k$. In consequence, the finger cannot grasp any object with the upper phalanges since they cannot apply forces. This situation is similar to the condition of existence of matrix $\mathbf{T}$. Such situations should be avoided through suitable design, so that $h_i,\ i > 1$ will always be positive, and $h_i + l_{i-1} \neq 0,\ i > 1$.

B. Discussion on the Positive Definiteness of the Forces

Most usual cases shall now be explicitly given and studied. The following results have been verified using classical static analysis (free body diagrams). For $n = 2$, one has

$$\mathbf{J} = \begin{bmatrix} k_1 & 0 \\ k_2 + l_1\cos\theta_2 & k_2 \end{bmatrix} \tag{27}$$

$$\mathbf{T} = \begin{bmatrix} 1 & -\frac{h}{h+l_1} \\ 0 & 1 \end{bmatrix} \tag{28}$$

$$\mathbf{f} = \begin{bmatrix} \frac{l_1(k_2 - h\cos\theta_2)Ta}{k_1k_2(h+l_1)} - \frac{(k_2 + l_1\cos\theta_2)T_2}{k_1k_2} \\ \frac{hT_a}{k_2(h+l_1)} + \frac{T_2}{k_2} \end{bmatrix}. \tag{29}$$

And for $n = 3$

$$\mathbf{J} = \begin{bmatrix} k_1 & 0 & 0 \\ k_2 + l_1C_{\theta_2} & k_2 & 0 \\ k_3 + l_1C_{\theta_2\theta_3} + l_2C_{\theta_3} & k_3 + l_2C_{\theta_3} & k_3 \end{bmatrix} \tag{30}$$

$$\mathbf{T} = \begin{bmatrix} 1 & -\frac{h_2}{h_2+l_1} & -\frac{h_2h_3}{(h_2+l_1)(h_3+l_2)} \\ 0 & 1 & 0 \\ 0 & 0 & 1 \end{bmatrix} \tag{31}$$

$$\mathbf{f} = \begin{bmatrix} \frac{l_1UT_a}{k_1k_2k_3(h_2+l_1)(h_3+l_2)} - \frac{(k_2+l_1\cos\theta_2)T_2}{k_1k_2} + \frac{l_1VT_3}{k_1k_2k_3} \\ \frac{h_2l_2(k_3 - h_3\cos\theta_3)T_a}{k_2k_3(h_2+l_1)(h_3+l_2)} + \frac{T_2}{k_2} - \frac{(k_3 + l_2\cos\theta_3)T_3}{k_2k_3} \\ \frac{h_2h_3T_a}{k_3(h_2+l_1)(h_3+l_2)} + \frac{T_3}{k_3} \end{bmatrix} \tag{32}$$

with

$$C_{\theta_i\theta_j} = \cos\left(\sum_{l=i}^{j}\theta_l\right). \tag{33}$$

The coefficients in (32) are defined as

$$U = k_2k_3h_3 + k_2k_3l_2 - h_2k_3l_2\cos\theta_2 + h_2h_3l_2\cos\theta_2\cos\theta_3 - h_2h_3k_2\cos(\theta_2+\theta_3) \tag{34}$$

$$V = l_2\cos\theta_2\cos\theta_3 + k_3\cos\theta_2 - k_2\cos(\theta_2+\theta_3). \tag{35}$$

These expressions allow the determination, for a set of geometric parameters, of the contact situations defined by the pair $(\mathbf{k}^*, \boldsymbol{\theta}^*)$ with

$$\mathbf{k}^* = \begin{bmatrix} k_2 \\ k_3 \\ \cdots \\ k_n \end{bmatrix} \quad \text{and} \quad \boldsymbol{\theta}^* = \begin{bmatrix} \theta_2 \\ \theta_3 \\ \cdots \\ \theta_n \end{bmatrix} \tag{36}$$

that allow full positiveness of the vector $\mathbf{f}$. The set of these contact situations corresponds to the stable part of the space spanned by the contact situations pair $(\mathbf{k}^*, \boldsymbol{\theta}^*)$, namely, the space of contact configurations. Stable grasps as we referred to should not be confused with form- or force-closure as usually defined in the literature. In this paper, a stable grasp is a contact situation pair which corresponds to a vector $\mathbf{f}$ where no component is negative. Again, this paper tries to characterize the finger itself, independently from the object being grasped. If springs are neglected, expressions of the latter vectors become most simple. θ_1 is obviously absent from the expressions because rotation about this axis leaves the mechanism in the same kinematic configuration (the finger is rotated as one single rigid body). It can also be shown that signs of elements of $\mathbf{f}$ are independent of k_1; the proof is, however, more cumbersome and relies on the general inverse calculus by means of cofactors.

The limit between the zones where all elements of $\mathbf{f}$ are positive and the rest of the space is, therefore, a $(2n-3)$ hypersurface in the contact situation space. Therefore, it is impossible to completely visualize this frontier (between all positive component space and its complement), even in the three-phalanx case. Note, for example, that for the set of parameters presented in Table I (which corresponds approximately to the parameters used in our prototypes of underactuated hands [27]), the volume of the stable three-phalanx grasps is approximately 14% of the whole space of contact configurations (a section of the configuration space is shown in Fig. 4), assuming this space to be bounded by a hyperparallelepiped defined by $0 < k_i < l_i$, $i > 0$ and $-\pi < \theta_i < \pi$, $i > 0$. This can seem abnormally small but, one should remember that full-phalanx grasps correspond only to a part of the whole possible grasps. That is, fewer-than-n-phalanx grasps can also be stable, as will be detailed in Section V. Furthermore, the stable contact situations are almost always located in the intuitive useful workspace. For example, if one changes the angular limits to $0 < \theta_i < \pi/2$, $i > 0$, the percentage of stable three-phalanx grasps jumps to approximately 32%. One should also note that even if the contact situation allows $\mathbf{f}$ to be fully definite, the ratios between the components of this vector are independent of the actuator torque. Thus, in each contact situation, span $(\mathbf{f})$ is of dimension one, and can be parameterized by T_a. One cannot modify the ratios between the components of $\mathbf{f}$ without changing the contact situation. For a fully actuated finger, span $(\mathbf{f})$ is of dimension n.

TABLE I
GEOMETRIC PARAMETERS

Set	l_1	l_2	l_3	ψ	a_1	b_1	c_1	a_2	b_2	c_2
1	61	41	38	$\pi/2$	38	58	16	38	58	16

The conditions for f_i to become zero, which can be considered as the edge of positiveness, become more complicated as i decreases. For example

$$f_n = 0 \Leftrightarrow \prod_{i=2}^{n} h_i(h_i + l_{i-1}) = 0 \tag{37}$$

$$f_{n-1} = 0 \Leftrightarrow \begin{cases} g_{n-1} = k_n - h_n\cos\theta_n = 0 \\ \text{or} \\ \prod_{i=2}^{n-1} h_i(h_i + l_{i-1}) = 0 \end{cases} \tag{38}$$

$$f_{n-2} = 0 \Leftrightarrow \begin{cases} g_{n-2} = h_{n-1}l_{n-1}g_{n-1}\cos\theta_{n-1} \\ -k_{n-1}k_n(h_n + l_{n-1}) \\ +h_{n-1}h_nk_{n-1}\cos(\theta_{n-1}+\theta_n) = 0 \\ \text{or} \\ \prod_{i=2}^{n-2} h_i(h_i + l_{i-1}) = 0 \end{cases} \tag{39}$$

$$f_{n-3} = 0 \Leftrightarrow \begin{cases} g_{n-3} = 0 = \\ -h_{n-2}h_{n-1}k_{n-2}l_{n-2}g_{n-1}C_{\theta_{n-2}\theta_{n-1}} \\ -k_{n-2}k_{n-1}(h_{n-1} + l_{n-2})(h_n + l_{n-1}) \\ +h_{n-2}h_{n-3}h_nk_{n-2}k_{n-1}C_{\theta_{n-2}\theta_{n-1}\theta_n} \\ \text{or} \\ \prod_{i=2}^{n-3} h_i(h_i + l_{i-1}) = 0. \end{cases} \tag{40}$$

The first condition on f_{n-1}, namely, g_{n-1}, has a simple geometrical meaning, i.e., the contact point is located on the equilibrium position of the last phalanx [26] [Fig. 5(b)]. However, to the best of the knowledge of the authors, higher order cases have no simple interpretation and can correspond to situations where intuitively, one would expect that a full-phalanx grasp is stable [Fig. 5(c)]. Illustration of configurations where one or more forces become negative are shown in Fig. 5.

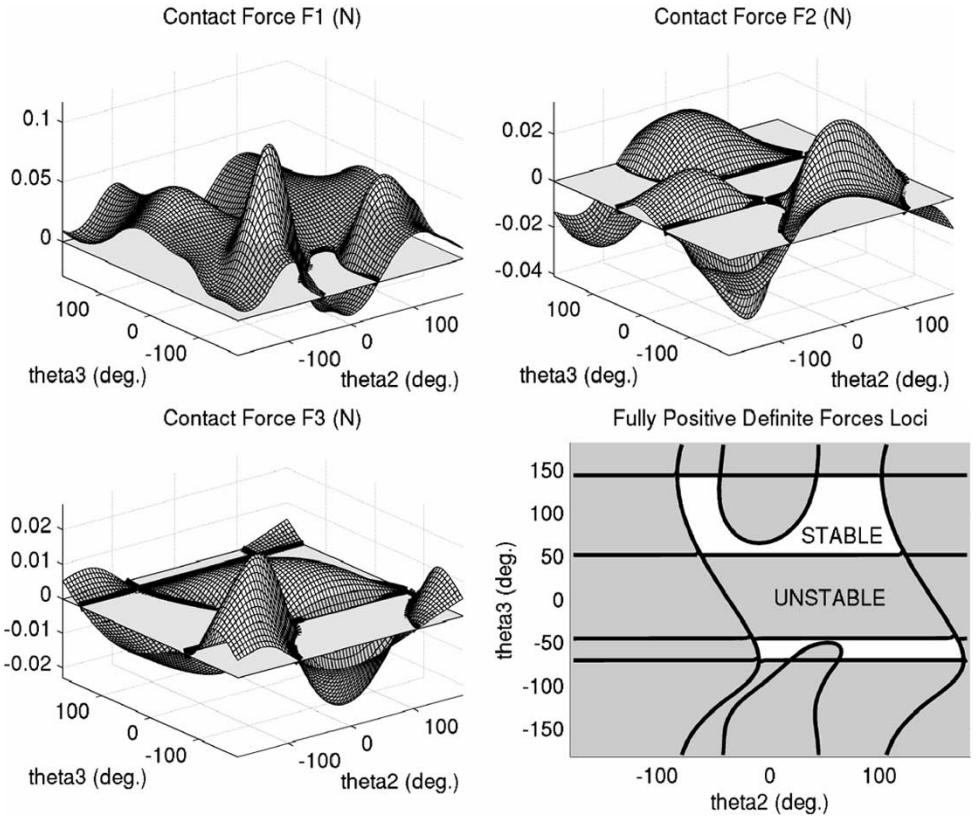

Fig. 4. Contact forces and associated stability loci ($k_2 = l_2/2$ and $k_3 = l_3/2$). Each force component is shown with the plane $f_i = 0$ in grey, intersections with the latter are outlined.

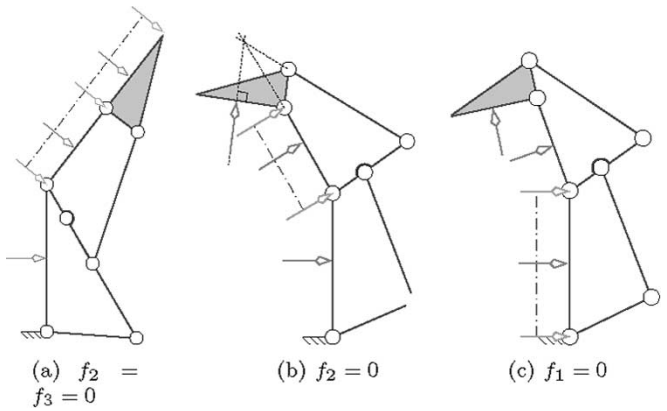

Fig. 5. Contact situations where one or more forces vanish (parameter set 1). If k_i exists, it is assumed that $k_i = l_i/2$. Vanishing forces are indicated by dashed lines.

A remarkable result is that the vanishing of f_n is most rare, because it can only happen when one X_i, $i > 1$ is zero, which can be prevented by means of mechanical limits or careful design. One can also remark that if one and only one f_i is zero for a given $\boldsymbol{\theta}^*$, there is an implicit relationship between the k_j's for $j > i$ only. If more f_i's are zero, one has a set of implicit equations that must be satisfied by certain components of the contact situation pair. The latter can have one, many, or no solutions, determining if this equilibrium configuration is possible. To obtain a final stable grasp with the general n-phalanx finger, one should have a contact situation $(\mathbf{k}^*, \boldsymbol{\theta}^*)$ where the contact force vector $\mathbf{f}$ has only positive components (however, not strictly). It is trivial to demonstrate that such situations are a subset of the set described by $f_n \geq 0$, meaning that the finger cannot be in equilibrium if the last phalanx is not. This simple statement yields more consequences than it seems, as to ensure the final stability of the grasp, one has to obtain a stable last phalanx. Thus, one can design the last phalanx to obtain an optimally stable design [26]. That way, under the assumption that the variation of position of point O_{n-1} is negligible and no internal periodic mobility is possible, contact made with the last phalanx will never be lost inside the finger workspace, and such an initial contact will tend to converge to a stable contact situation. The evolution of the contact situation trajectory can be rather complex, depending on the geometry of the grasped object and the dynamic properties of the phalanges. Contacts can be made, lost, remade, etc., during the grasping sequence. Nevertheless, if one uses an optimal last phalanx design, a stable configuration will be attained under the assumptions previously stated. It should be noted that the second type of unstable frontier described in [26] should be avoided at any cost, because it can lead to a *roll-back phenomenon*, where the last phalanx slides against the object with a continuous closing motion, resulting in a situation where the finger grasps nothing but itself (Fig. 6). This phenomenon is the n-phalanx generalization of the ejection phenomenon presented in [20]. The design presented in [20] insists on the mechanical joint limits of $0 < \theta_n < \pi/2$ to avoid the latter type of ejection, which is the reason why we have previously named this range "useful workspace." Mechanical limits are key elements in the design of underactuated fingers considering stability issues, because they limit the shape adaptation to

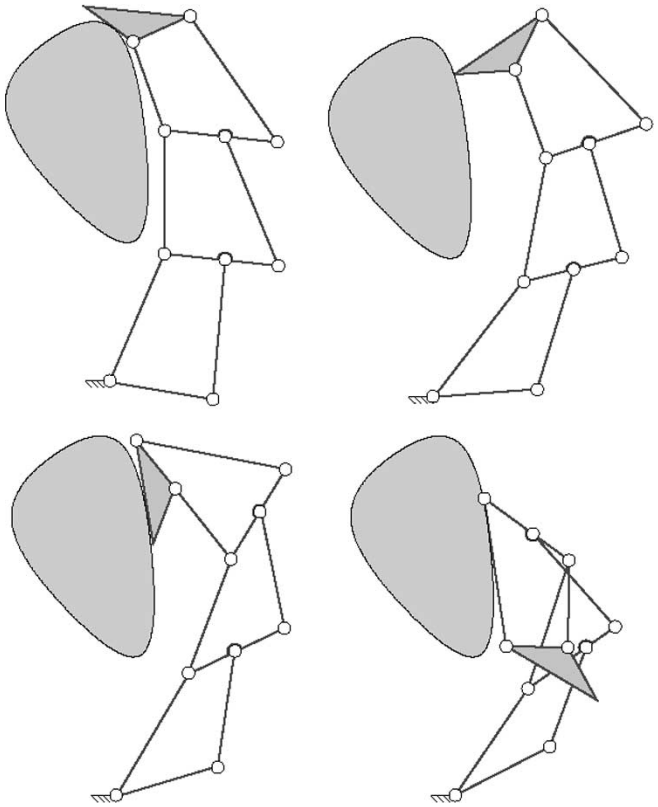

Fig. 6. Roll-back phenomenon.

reasonable configurations (thus avoiding ejection). In the worst case where all joints except the first one are locked, the finger simply acts as a basic rotational gripper (with a quite complex shape), but still can firmly grasp the object. From that point of view, underactuated hands could be considered more like grippers with shape adaptation than traditional robotic hands.

Finally, one can also characterize the capability of the underactuated finger to create full-phalanx grasps with an index

$$\mu = \frac{\int_W \delta(\mathbf{k}^*, \boldsymbol{\theta}^*) d\mathbf{k}^* d\boldsymbol{\theta}^*}{\int_W d\mathbf{k}^* d\boldsymbol{\theta}^*} \tag{41}$$

where $\delta(\mathbf{k}^*, \boldsymbol{\theta}^*)$ is a Kronecker-like symbol for positiveness of vector $\mathbf{f}$ that eliminates non-whole-phalanx grasps

$$\delta(\mathbf{k}^*, \boldsymbol{\theta}^*) = \begin{cases} 1, & \text{if } f_i > 0 \,\forall\, i > 0 \\ 0, & \text{otherwise} \end{cases} \tag{42}$$

and W is the workspace of the finger in terms of $(\mathbf{k}^*, \boldsymbol{\theta}^*)$, i.e., the hyperparallelepiped defined by $0 < k_i < l_i$, $i > 0$ and $-\pi < \theta_i < \pi$, $i > 0$ or $0 < \theta_i < \pi/2$, $i > 0$ (to be preferred). This index physically represents the percentage of the workspace that is achievable by full-phalanx grasps, namely, whole-hand grasping workspace. One shall modify the index definition to obtain a measure of how far one is to lose contact with one phalanx by including a "distance" from the vanishing of the smallest component, i.e.,

$$\eta = \frac{\int_W \min_i(f_i) \delta(\mathbf{k}^*, \boldsymbol{\theta}^*) d\mathbf{k}^* d\boldsymbol{\theta}^*}{\int_W T_a d\mathbf{k}^* d\boldsymbol{\theta}^*}. \tag{43}$$

One can also use an index based on the grasp-forces distribution to provide the grasp with roughly equally distributed contact forces, such as (based on [34], slightly modified)

$$I = \frac{\int_W \frac{\sum_i^n f_i}{\max_i(f_i)} \delta(\mathbf{k}^*, \boldsymbol{\theta}^*) d\mathbf{k}^* d\boldsymbol{\theta}^*}{n \int_W d\mathbf{k}^* d\boldsymbol{\theta}^*}. \tag{44}$$

Numerical values of the latter indexes will be presented in Section IV-D.

IV. Other Transmission Mechanisms

The benefit of the method presented in this paper is that it allows one to obtain very quickly the expression of the contact forces developed by an underactuated finger. This can be especially useful if different mechanisms are considered, matrix $\mathbf{J}$ is independent of the type of the transmission, and only the elements of matrix $\mathbf{T}$ need to be modified. A method to express the coefficients of $\mathbf{T}$ follows. One has to remember the general form of (15) obtained by superposition, i.e.,

$$\dot{\theta}_{a_{i-1}} = \dot{\theta}_{i-1} + x_i \dot{\theta}_{a_i} \tag{45}$$

where x_i is the transmission factor of the ith stage. The latter equation means that the velocity output of each stage is the input of the next stage (Fig. 3 illustrates this concept). To obtain the factor x_i, one simply has to virtually "lock" θ_{i-1} and determine the ratio between $\dot{\theta}_{a_i}$ and $\dot{\theta}_{a_{i-1}}$, which can be obtained for any mechanism. Most usual transmissions (e.g., gears, pulleys) are already well known. Once this factor is defined, a recursive scheme can be easily derived from (15), and therefore, the coefficients X_i can be written as

$$\begin{cases} X_1 = 1 \\ X_j = -\prod_{i=2}^{j} x_i, \quad j = 2 \ldots n. \end{cases} \tag{46}$$

Finally, expressions for the contact forces are obtained by (22) where the inversion of both $\mathbf{J}$ and $\mathbf{T}$ matrices is needed. In the following sections, examples of usual transmission mechanisms will be given. Notice that different types of mechanisms can be mixed in the same finger without changing the method.

A. Double-Stage Mechanism

The so-called double-stage mechanism, i.e., a mechanism similar to the one represented in Fig. 2 but with two consecutive phalanges merged into a single one, has been considered for compactness [18]. Analyzing such mechanisms is very similar to the initial study, the matrix $\mathbf{J}$ remains unchanged since the finger is still planar (keeping in mind that phalanx lengths should be adjusted), and only revolute joints are used. Matrix $\mathbf{T}$ becomes

$$\mathbf{T}^T = \begin{bmatrix} 1 & \mathbf{0}_{n-1}^T \\ -\frac{h_2 h_3}{(h_2 + l_1)(h_3 + l_2)} & \\ \cdots & \mathbf{1}_{n-1} \\ -\prod_{i=1}^{n} \frac{h_{2i} h_{2i+1}}{(h_{2i} + l_{2i-1})(h_{2i+1} + l_{2i})} & \end{bmatrix}. \tag{47}$$

It corresponds simply to locking every even-numbered joint from the previous design to zero degree. The expression of the matrix is straightforward and can be used to design a particular

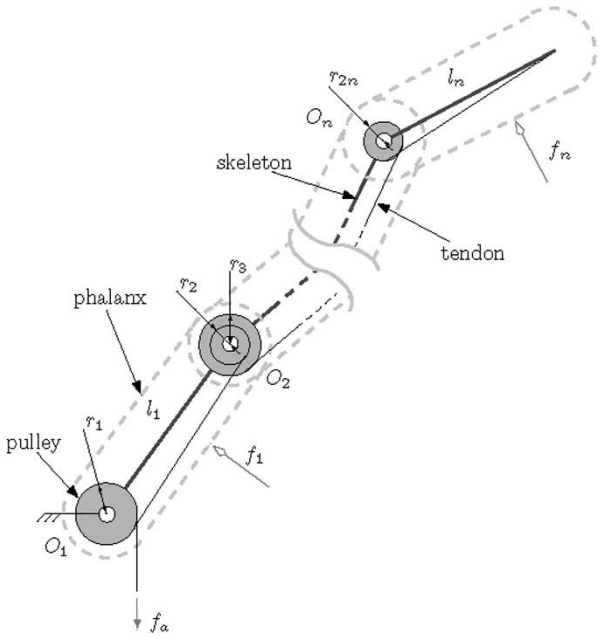

Fig. 7. Tendon-actuated finger.

finger with a specific desired grasp-force distribution. By using two stages instead of one, one can obtain specific ratios without having large a_i and c_i link lengths. Thus, this mechanism will indeed generally lead to more compact designs. However, such designs will also have some drawbacks, such as the limited space available for sensors.

B. Tendon-Pulley Transmission

A legacy of the tradition in robot finger actuation, i.e., a tendon-actuated finger, is now studied. Such designs have already been used in underactuated fingers [13], [17], [22], [35]. The proposed layout is shown in Fig. 7. The expression of matrix $\mathbf{J}$ remains again unchanged. Matrix $\mathbf{T}$ can be simply expressed as

$$\mathbf{T}^T = \begin{bmatrix} 1 & \mathbf{0}_{n-1}^T \\ -\dfrac{r_2}{r_1} & \\ -\dfrac{r_2 r_4}{r_1 r_3} & \\ \cdots & \mathbf{1}_{n-1} \\ -\prod_{i=1}^{n} \dfrac{r_{2i}}{r_{2i-1}} & \end{bmatrix} \tag{48}$$

where r_{2i-1} and r_{2i} for $i > 0$ are, respectively, the radius of the pulley located at the base and the end of the ith phalanx. Note that, in this case, the latter matrix is constant for any configuration of the finger, as opposed to what was obtained in the analysis presented above for fingers actuated with linkages. One can again proceed with the expression of the contact force vector as

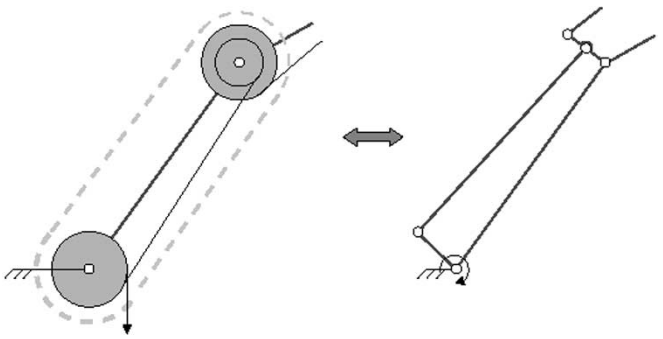

Fig. 8. Equivalence between pulley-tendon and four-bar transmission.

presented in (22). An interesting result arises if the pulley radius ratio is constant, i.e.,

$$\frac{r_{2i}}{r_{2i-1}} = \alpha \quad i > 0. \tag{49}$$

Usually, $\alpha < 1$ for compactness purposes. The latter expression considerably simplifies the expression of matrix $\mathbf{T}$. The expression of the last phalanx forces can then be expressed as

$$\begin{cases} f_n = \dfrac{\alpha^{n-1}}{k_n} T_a \\ f_{n-1} = -\dfrac{\alpha^{n-2}(k_n(\alpha-1) + \alpha l_{n-1}\cos\theta_n)}{k_{n-1}k_n} T_a \end{cases} \tag{50}$$

with $T_a = r_1 f_a$. Similar to the previous study, conditions for the forces to become zero are implicit functions that cannot be easily solved. Interestingly, the contact force on the last phalanx is only the function of the ratio α and the location of the corresponding contact k_n, not the configuration of the finger itself. Moreover, one can define an equilibrium point [26] for this mechanism as

$$k_n = e_n = \frac{\alpha}{1-\alpha} l_{n-1}\cos\theta_n. \tag{51}$$

Furthermore, note that the limit case where $\alpha = 1$ is again an almost always unstable design (equilibrium point pushed to infinity) for the two-phalanx finger, like its mechanical "evil twin," the parallelogram [26]: both have the exact same condition for positiveness! Similar to what was obtained in Section III-B, a tendon-actuated finger with pulley radii equivalent to link lengths, i.e., $r_{2i-1} = a_i$ and $r_{2i} = c_i$, has a possible stable three-phalanx grasp occurrence of approximately 56%, to be compared with the 14% of the mechanism first studied. If limits are placed on elements of $\boldsymbol{\theta}$, similar to what was done in Section III-B, that percentage drops to approximately 41%, which is still superior to the mechanical linkage. Thus, for small forces and with appropriate control to compensate elasticity and friction, this mechanism can be very efficient, as, for instance, for lightweight prosthetic devices. The kinematic similarity between both mechanisms is pointed out with our analysis technique, highlighting the inherent generality of the presented method. Instantaneous equivalence is illustrated in Fig. 8.

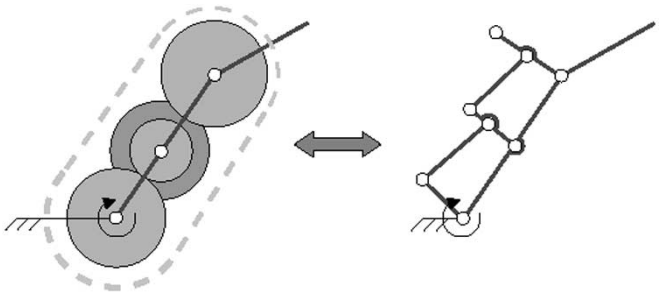

Fig. 9. Equivalence between gears and four-bar transmission (gears are represented by their primitive circles).

TABLE II
CHARACTERISTIC INDEXES

Transmission	n	μ	η	I
linkages	3	0.32	0.0011	0.17
linkages	2	0.43	0.0051	0.21
pulley-tendons	3	0.41	0.0019	0.24
pulley-tendons	2	0.53	0.0058	0.27
gears	2	0.63	0.0037	0.33
double-stage	2	0.64	0.0035	0.32

C. Gears

Consider that instead of tendons, one has a gear train connecting the principal gears located on the axis of the fingers. With such a mechanism, matrix $\mathbf{T}$ becomes

$$\mathbf{T}^T = \begin{bmatrix} 1 & \mathbf{0}_{n-1}^T \\ \dfrac{N_2 N_2^{1\star}}{N_1 N_2^1} & \\ -\dfrac{N_2 N_2^{1\star} N_4 N_4^{3\star}}{N_1 N_2^1 N_3 N_4^3} & \\ \cdots & \mathbf{1}_{n-1} \\ -\prod_{i=1}^{n} \dfrac{N_{2i} N_{2i}^{2i-1\star}}{N_{2i-1} N_{2i}^{2i-1}} & \end{bmatrix} \tag{52}$$

where N_{2i-1} and N_{2i} are, respectively, the number of teeth of the gear located at the base and the end of the ith phalanx. Both gears are connected through a train that can be described by two equivalent gears with tooth ratio $N_{2i}^{2i-1*}/N_{2i}^{2i-1}$, that is, the gear with N_{2i}^{2i-1} teeth is in contact with the gear N_{2i-1}, which is rigidly connected with gear N_{2i}^{2i-1*}, which itself finally transmits motion to gear N_{2i}. Note that this form is very similar to the double-stage mechanism presented in Section IV-A. In fact, this mechanism is to pulleys and tendons what double-stage is to the four-bar mechanism. A comparison is again illustrated in Fig. 9.

D. Comparison

To compare the different mechanisms presented in the previous sections, one can use the indexes presented in (41), (43), and (44). Results are presented in Table II. In order to obtain comparable indexes, equivalence between link lengths, pulley radii, etc., are established with the same rule as in Section IV-B and with the parameters defined in Table I. When only two phalanges are considered, geometrical parameters will correspond to the last two phalanges in the latter table. The workspace used is defined by $0 < k_i < l_i,\ i > 0$ and $0 < \theta_i < \pi/2,\ i > 0$.

It can be seen that in general, tendon-actuated fingers have better overall performances than linkage-actuated ones. This is due to the fact that they do not suffer from mechanical singular configurations (for example, when three points of the transmission mechanism are on the same line, see Section III-B). This is not the case with multiple-stage fingers, because such singular configurations become most rare if they exist at all, since both stages contribute to attaining the same kinematic configuration. However, larger forces can be applied with linkages than with tendons, since power transmission is performed through rigid bodies, resulting in very firm grasps. With more phalanges, one tends to achieve more adaptive grasps, but it becomes less likely that all phalanges simultaneously perform the grasp.

V. LESS-THAN-N PHALANX GRASPS

In order for a less-than-n phalanx grasp to be stable, every phalanx in contact with the object should have a corresponding force strictly positive. For phalanges not in contact with the object, the corresponding generated forces, defined in (22), should be zero, since the latter forces can also be seen as the external forces needed to counter the actuation torque; equilibrium is implicitly assumed by (1). Thus, the relationships discussed in Section III-B for positiveness of forces also give us the equilibrium conditions for less-than-n phalanx grasps. For example, if one wants to know under which conditions a stable grasp can be achieved with no contact on phalanx, say $n-1$, one has to satisfy the condition

$$\begin{cases} f_j > 0, & j \neq n-1 \\ g_{n-1} = 0. \end{cases} \tag{53}$$

Such conditions are of greater importance than it seems at first glance, since, as it has been shown, only part of the finger contact situation space is stable with full-phalanx stable grasps. Thus, full-phalanx grasps are only a subset of the possible stable grasp contact configurations. Many questions remain unanswered to characterize the behavior of the finger, e.g., is there a global index that would allow us to describe the overall stability of the finger? Generalization of the ejection phenomenon seems a promising way to characterize the stability of an underactuated finger, but this theory should be extended to cases where the hypotheses presented in Section III-B are relaxed. Moreover, nontrivial less-than-n phalanx contact equilibrium is possible, nontrivial, meaning with nonsimple geometrical relationships, like two links on the same line. Thus, it is theoretically possible to fully constrain a general n-DOF finger with a single contact in such nontrivial configurations.

VI. CONCLUSIONS

This paper has presented and analyzed the force capabilities of underactuated fingers. The main contribution of this paper is the introduction of matrices $\mathbf{J}$ (Jacobian) and $\mathbf{T}$ (Transmission). These matrices allow immediate characterization of the finger, provide the expressions of contact forces developed by the finger, lead to considerations on equilibrium with any number

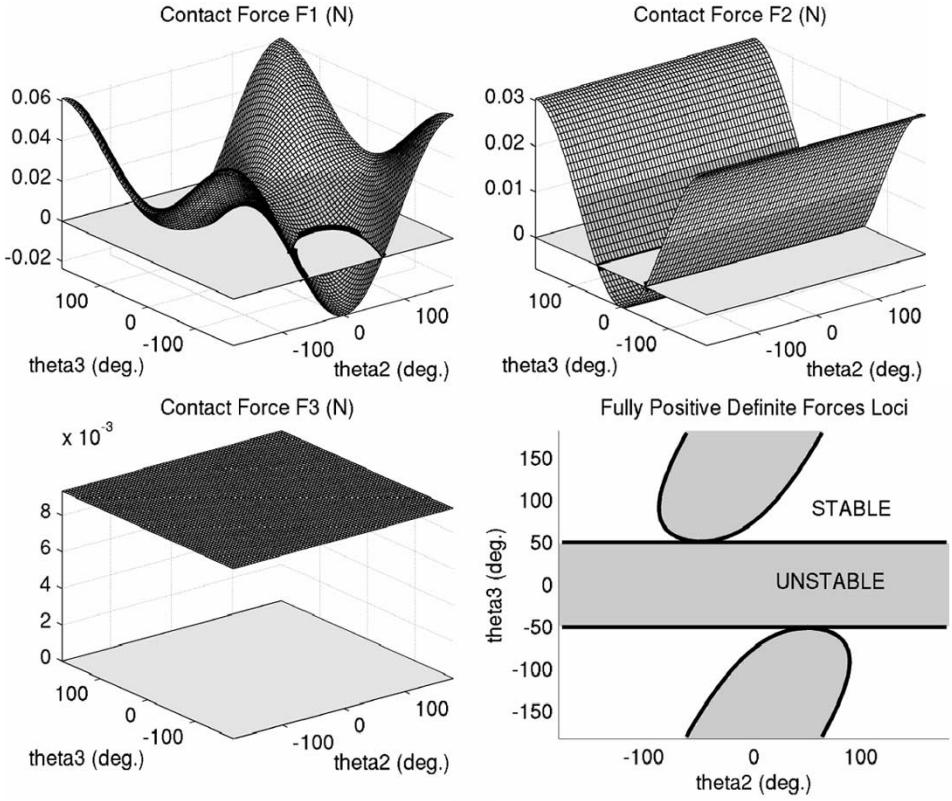

Fig. 10. Tendon-actuated mechanism, contact forces, and stability loci ($k_2 = l_2/2$ and $k_3 = l_3/2$). Each force component is shown with the plane $f_i = 0$ in grey, intersections with the latter are outlined.

of phalanges in contact, and provide tools for comparison between different designs. Such comparisons can be very useful to choose a particular design of underactuated finger. However, one should keep in mind other considerations that are not easily mathematically quantifiable. For example, friction and elasticity can eliminate tendon-actuated fingers, despite their good performance indexes. Furthermore, if theoretically, an infinite number of phalanges is ideal for grasping, since such a finger would tend to approach the spatial complement of the shape of the object, which is the perfect grasper, practical considerations of cost and complexity of the design limit the number of phalanges to generally three or four, at most. Hence, the authors believe that the tools presented in this paper can help refine underactuated finger designs in terms of geometric parameters, although the general layout of the finger remains application driven. In order to properly design underactuated fingers, one should be aware of the ejection phenomenon, in order to achieve stable grasps and phalanx force distribution, avoiding weak last phalanges that cannot ensure sufficient force to secure the grasp. Material not included here because of lack of space and under current investigation includes the in-depth study of a three-phalanx finger considering friction, geometry of the contact, and optimal phalanx force distribution.

ACKNOWLEDGMENT

The first author expresses his most grateful thanks to the original designer of our prototypes of underactuated hands, T. Laliberté, for providing him with such stimulating material. *Merci*!

REFERENCES

[1] T. Okada, "Computer control of multijointed finger system for precise object handling," *IEEE Trans. Syst., Man, Cybern.*, vol. SMC-12, pp. 289–299, Feb. 1982.

[2] J. K. Salisbury and J. J. Craig, "Articulated hands: Force control and kinematic issues," *Int. J. Robot. Res.*, vol. 1, no. 1, pp. 4–17, 1982.

[3] S. C. Jacobsen, E. K. Iversen, D. F. Knutti, R. T. Johnson, and K. B. Biggers, "Design of the Utah/MIT dextrous hand," in *Proc. IEEE Int. Conf. Robotics and Automation*, San Francisco, CA, 2001, pp. 1520–1532.

[4] G. A. Bekey, R. Tomovic, and I. Zeljkovic, *Control Architecture for the Belgrade/USC Hand in Dextrous Robot Hands*. New York: Springer-Verlag, 1999.

[5] N. T. Ulrich, "Methods and Apparatus for Mechanically Intelligent Grasping," U.S. Patent 4 957 320, Sept. 18, 1990.

[6] H. Liu, P. Meusel, J. Butterfass, A. Knoch, and G. Hirzinger, "DLR's multisensory articulated hand, part I-II," in *Proc. IEEE Int. Conf. Robotics and Automation*, Leuven, Belgium, May 1998, pp. 2087–2093.

[7] J. Butterfass, M. Grebenstein, H. Liu, and G. Hirzinger, "DLR-hand II: Next generation of a dextrous robot hand," in *Proc. IEEE Int. Conf. Robotics and Automation*, Seoul, Korea, May 2001, pp. 109–114.

[8] J. P. Gazeau, S. Zeghloul, M. Arsicault, and J. P. Lallemand, "The LMS hand: Force and position control in the aim of the fine manipulation of objects," in *Proc. IEEE Int. Conf. Robotics and Automation*, Seoul, Korea, May 2001, pp. 2642–2648.

[9] M. A. Diftler and R. O. Ambrose, "Robonaut: A robotic astronaut assistant," in *Proc. 6th Int. Symp. Artificial Intelligence and Robotics and Automation in Space: i-SAIRAS 2001*, Saint-Hubert, QC, Canada, June 2001.

[10] A. Bicchi and V. Kumar, "Robotic grasping and contact: A review," in *Proc. IEEE Int. Conf. Robotics and Automation*, vol. 1, Apr. 2000, pp. 348–353.

[11] A. Bicchi, "Hands for dexterous manipulation and powerful grasping: A difficult road toward simplicity," *IEEE Trans. Robot. Automat.*, vol. 16, pp. 652–662, Dec. 2000.
[12] D. L. Akin, C. R. Carignan, and A. W. Foster, "Development of a four-fingered dexterous robot end-effector for space operations," in *Proc. IEEE Int. Conf. Robotics and Automation*, Washington, DC, May 2002, pp. 2302–2308.
[13] J. D. Crisman, C. Kanojia, and I. Zeid, "Graspar: A flexible, easily controllable robotic hand," *IEEE Robot. Automat. Mag.*, pp. 32–38, June 1996.
[14] L. Biagiotti, C. Melchiorri, and G. Vassura, "Control of a robotic gripper for grasping objects in no-gravity conditions," in *Proc. IEEE Int. Conf. Robotics and Automation*, Seoul, Korea, May 2001, pp. 1427–1432.
[15] G. Figliolini and M. Ceccarelli, "A novel articulated mechanism mimicking the motion of index fingers," *Robotica*, vol. 20, pp. 13–22, 2002.
[16] N. Dechev, W. L. Cleghorn, and S. Naumann, "Multiple finger, passive adaptive grasp prosthetic hand," *Mech. Mach. Theory*, vol. 36, pp. 1157–1173, 2001.
[17] S. Hirose and Y. Umetani, "The development of soft gripper for the versatile robot hand," *Mech. Mach. Theory*, vol. 13, pp. 351–358, 1978.
[18] H. Shimojima, K. Yamamoto, and K. Kawakita, "A study of grippers with multiple degrees of mobility," *JSME Int. J.*, no. 261, pp. 515–522, 1987.
[19] M. Rakic, "Multifingered robot hand with self-adaptability," *Robot. Comput.-Integrat. Manuf.*, vol. 3, no. 2/3, pp. 269–276, 1989.
[20] T. Laliberté and C. Gosselin, "Simulation and design of underactuated mechanical hands," *Mech. Mach. Theory*, vol. 33, no. 1/2, pp. 39–57, 1998.
[21] B. Kennedy, "Three-fingered robot hand with self-adjusting grip," *NASA Tech. Briefs*, p. 59, Dec. 2001.
[22] B. Massa, S. Roccella, M. C. Carrozza, and P. Dario, "Design and development of an underactuated prosthetic hand," in *Proc. IEEE Int. Conf. Robotics and Automation*, Washington, DC, May 2002, pp. 3374–3379.
[23] Y. Bar-Cohen, T. Xue, M. Shahinpoor, and S.-H. Lih, "Robot hands with electroactive polymer fingers," *NASA Tech. Briefs*, Oct. 1998.
[24] S. Schulz, C. Pylatiuk, and G. Bretthauer, "A new ultralight anthropomorphic hand," in *Proc. IEEE Int. Conf. Robotics and Automation*, Seoul, Korea, May 2001, pp. 2437–2441.
[25] J. S. Pettinato and H. E. Stephanou, "Manipulability and stability of a tentacle-based robot manipulator," in *Proc. IEEE Int. Conf. Robotics and Automation*, Scottsdale, AZ, May 1989, pp. 458–463.
[26] L. Birglen and C. M. Gosselin, "On the force capabilities of underactuated fingers," in *Proc. IEEE Int. Conf. Robotics and Automation*, vol. 1, Taipei, Taiwan, May 2003, pp. 1139–1145.
[27] C. Gosselin and T. Laliberté, "Underactuated Mechanical Finger With Return Actuation," US Patent 5,762,390, June 9, 1998.
[28] I. A. Bonev, D. Zlatanov, and C. Gosselin, "Singularity analysis of 3-DOF planar parallel mechanisms via screw theory," *ASME J. Mech. Des.*, vol. 125, no. 1, Sept. 2003.
[29] K. H. Hunt, *Kinematic Geometry of Mechanisms*. Oxford, U.K.: Oxford Univ. Press, 1978.
[30] R. L. Norton, *Design of Machinery*. New York: McGraw-Hill, Inc., 1992.
[31] J. M. McCarthy, *Geometric Design of Linkages*. New York: Springer-Verlag, 2000.
[32] T. Yoshikawa, "Control algorithm for grasping and manipulation by multifingered robot hands using virtual truss model representation of internal force," in *Proc. IEEE Int. Conf. Robotics and Automation*, San Francisco, CA, Apr. 2000, pp. 369–376.
[33] M. T. Mason and J. K. Salisbury, *Robot Hands and the Mechanics of Manipulation*. Cambridge, MA: MIT Press, 1985.
[34] T. Laliberté and C. Gosselin. Development of a three-DOF underactuated finger. presented at *Proc. CCToMM Symp. Mechanisms, Machines, and Mechatronics*. [Online]. Available: http//www.me.uvic.ca/~ram/2001_CCToMM_Symposium/
[35] C. M. Seguna and M. A. Saliba, "The mechanical and control system design of a dexterous robotic gripper," in *Proc. IEEE Int. Conf. Electronics, Circuits, and Systems*, vol. 3, Sept. 2001, pp. 1195–1201.

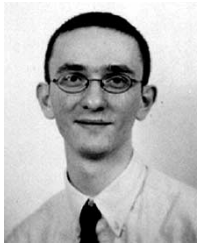

Lionel Birglen (S'00) received the B.Eng. degree in mechatronics from École Nationale Supérieure des Arts et Industries de Strasbourg, Strasbourg, France, in 2000. He is currently working toward the Ph.D. degree in mechanical engineering at the Robotics Laboratory, Université Laval, Québec, QC, Canada after an accelerated promotion from the M.Sc. level.

His work focuses on the kinematic analysis and control of complex mechanical hands and parallel manipulators, with a particular emphasis on force control and general theory of real-time control.

Mr. Birglen is a student member of ASME.

Clément M. Gosselin (S'88–M'89) received the B.Eng. degree in mechanical engineering from the Université de Sherbrooke, Sherbrooke, QC, Canada, in 1985, and the Ph.D. degree from McGill University, Montréal, QC, Canada in 1988.

In 1988, he accepted a post-doctoral fellowship from the French government and joined INRIA, Sophia Antipolis, France, for a year. In 1989, he joined the Department of Mechanical Engineering, Laval University, Quebec City, QC, Canada, where he has been a Full Professor since 1997. He has held a Canada Research Chair on Robotics and Mechatronics since January 2001. In 1995, he received a fellowship from the Alexander von Humboldt Foundation which allowed him to spend six months as a Visiting Researcher in the Institut für Getriebetechnik und Maschinendynamik, Technische Hochschule, Aachen, Germany. In 1996, he spent three months at the University of Victoria, Victoria, BC, Canada, for which he received a fellowship from the BC Advanced Systems Institute. His research interests are kinematics, dynamics, and control of robotic mechanical systems with a particular emphasis on the mechanics of grasping and the kinematics and dynamics of parallel manipulators and complex mechanisms. His work in the aforementioned areas has been the subject of several publications in international conferences and journals. He is the French language editor for the international journal *Mechanism and Machine Theory*.

Dr. Gosselin received the Gold Medal of the Governor General of Canada in 1985, the D. W. Ambridge Award from McGill University for the best thesis of the year in Physical Sciences and Engineering in 1988, and the I. Ω. Smith award from the Canadian Society of Mechanical Engineering in 1993. He is a member of the Institute for Robotics and Intelligent Systems (IRIS), one of the networks of the Canadian Centres of Excellence, and a member of the American Society of Mechanical Engineers (ASME) and the Canadian Committee for the Theory of Machines and Mechanisms (CCToMM).